ELSEVIER

Polymer 43 (2002) 4177–4183

polymer

www.elsevier.com/locate/polymer

Characterisation of injected EPBC plaques using the essential work of fracture (EWF) method

M.Ll. Maspoch*, J. Gámez-Pérez, A. Gordillo, M. Sánchez-Soto, J.I. Velasco

Centre Català del Plàstic (CCP-UPC), C/Colom 114, 08222 Terrassa, Spain

Received 3 January 2002; received in revised form 4 April 2002; accepted 8 April 2002

Abstract

The influence of processing induced morphology, thickness and ethylene content (EC) of different ethylene–propylene block copolymers on fracture properties has been studied using the essential work of fracture (EWF) method. To analyse the influence of EC, four different materials were chosen with 0, 5.5, 7.8, and 8.4% in weight EC. Each material was injected in three different thicknesses (1, 2 and 3 mm). The resulting plaques were tested using the EWF method in both main orientations; the melt flow direction and transverse to melt flow direction. Different fracture behaviours have been observed, some of them preventing the applicability of the EWF method. Polarised light microscopy observations have revealed the existence of a skin/core structure, which is reduced with an increase in thickness and EC.

Keywords: Essential work of fracture; Injection-moulding; Skin/core structure

1. Introduction

The development of new materials with improved mechanical properties allows the use of thinner components in technical pieces and objects of common use. However, fracture tests to characterise films and thin sheets still present some problems. Tearing tests do not provide information about intrinsic material properties. Furthermore, ductile films occurs in most cases of post-yielding fracture, so that the linear elastic fracture mechanics and elastic–plastic fracture mechanics approaches are no longer applicable.

In post-yielding fracture mechanics, the essential work of fracture (EWF) method has been successfully employed to describe the toughness of films and thin sheets made out of different ductile materials like metals [1], paper [2] or polymers [3–7] (and references therein). Although the references in the literature show the usefulness of EWF in polymeric materials, the influence of some variables (strain rate, thickness of the specimen, orientation, etc.) may limit its applicability. In the present work, ethylene–propylene block copolymers (EPBC) thin plaques obtained from injection-moulding were tested with the purpose of evaluating the influence of ethylene content (EC), thickness and orientation using the EWF method.

2. Theory

Cotterell and Reddel [8] developed the Broberg idea [9] of dividing the fracture energy (W_f) of a notched specimen into two terms:

$$W_f = W_e + W_p \tag{1}$$

The first one is the EWF (W_e). It is associated with the instability at the crack tip, where the true process of fracture occurs (process zone in Fig. 1), and is proportional to the specimen ligament area lt (where l is the ligament length and t thickness). The non-essential or plastic work of fracture (W_p) is related to the various energy dissipation mechanisms that occur in the proximity of the plastic zone and it is a volume-related term (proportional to tl^2)

$$W_f = w_e tl + \beta w_p tl^2 \tag{2}$$

$$w_f = w_e + \beta w_p l \tag{3}$$

where w_f, w_e and w_p are the specific terms and β is a shape factor for the plastic zone. According to Eq. (3), w_e and βw_p can be obtained from linear regression of a set of values represented in a diagram of specific total fracture energy vs. ligament length ($w_f - l$).

The specific essential work, w_e is in theory a material

* Corresponding author. Tel.: +34-93-783-70-22; fax: +34-93-784-18-27.

E-mail address: maria.lluisa.maspoch@upc.es (M.L. Maspoch).

0032-3861/02/$ - see front matter
PII: S0032-3861(02)00259-8

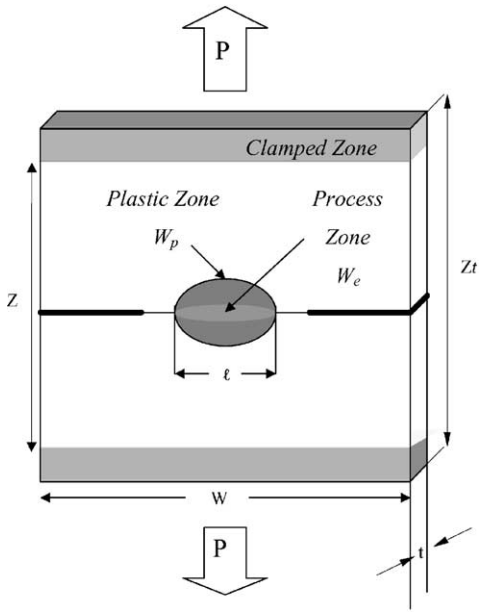

Fig. 1. DDENT specimen used in EWF tests, indicating the different zones involved during fracture.

constant dependent only on thickness and is equivalent to J_{IC} [4]. However, it is necessary that certain assumptions be satisfied in order to apply the EWF technique:

(a) The ligament must be fully yielded prior to crack propagation.
(b) Eq. (3) can only be applied under truly plane stress fracture. Hill's criterion [10] can be used to verify this argument.
(c) There must exist a common geometry of fracture for all ligament lengths, visible in the self-similarity of the curves in load–displacement (L–d) diagrams.

The ESIS protocol for EWF [11] recommends the use of deeply double edged notched tensile (DDENT) specimens and a set of limits for the ligament length

$$\mathrm{Max}(3t - 5\ \mathrm{mm}) < l < \min(W/3, 2r_p) \quad (4)$$

being

$$2r_p = (\pi/8)\left(Ew_e/\sigma_y^2\right) \quad (5)$$

where W is the width of the DDENT specimen, E and σ_y are, respectively, the elastic modulus and yield stress (obtained for the same material in tensile test and similar testing conditions).

3. Materials and experimental

The materials used in this study are a polypropylene homopolymer (H0) and three commercial EPBC with different EC (5.5, 7.4 and 12% in weight) named C1, C2 and C3, respectively. A more detailed characterisation of these materials can be found in a previous work [12].

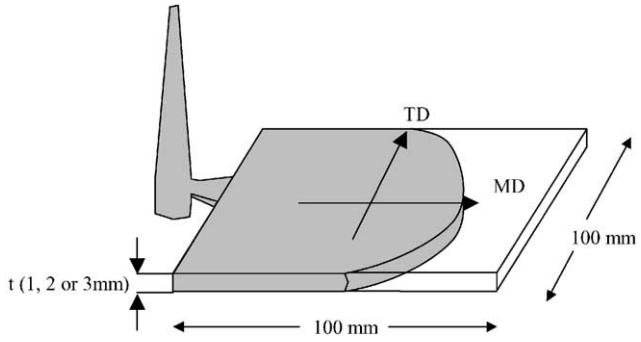

Fig. 2. Sketch of injected plaques indicating the main directions: MD and TD.

The materials were supplied as pellets. Next, they were injection-moulded in the form of plaques (Fig. 2) of different thickness ($t = 1$, 2 and 3 mm) using an injection-moulding machine Mateu & Solé-90Tm. The three moulds had fan gates and they were equipped with a cold-water cooling system (18 °C). Injection temperature was the same in all cases (230 °C). All plaques were conditioned at room temperature at least 48 h after injection prior to any test.

Tensile tests were performed according to ASTM D638. Type IV tensile dumb-bell specimens were machined from the plaques in both orientations, the melt flow direction (MD) and transverse to melt flow direction (TD). The yield stress σ_y (as the maximum stress) and the elastic modulus (F) were calculated from the engineering stress–strain curves.

DDENT specimens using all the injected plaque were prepared. The dimensions of the specimens were $W = 100$ mm, total length $Z_t = 100$ mm and distance between grips $Z = 70$ mm (Fig. 1). Initial notches were made with a circular saw perpendicular to the tensile direction and sharpened with a fresh razor blade just before testing. Eighteen specimens with different ligament lengths (l) were prepared. The minimum ligament lengths were set in accordance with Eq. (4). The upper limit was set at 25 mm to avoid edge effects. In order to increase the accuracy, the ligament length was measured after testing with a travelling binocular lens microscope.

Tension loading was applied to DDENT specimens in the main directions, MD and TD, and the resulting load vs. displacement curves were recorded. The total fracture energy W_f was calculated from the area of the curves by numerical integration.

All tests were performed at controlled temperature of 23.5 ± 1 °C and at crosshead speed of 2 mm/min. The crosshead speed was chosen to be able to compare the results with other works done by our group with the same materials but obtained by cast extrusion with a thickness of about 0.1 mm [13,14].

4. Results

The different sets of tests to determine the fracture

parameters were named with a code indicating material, thickness and orientation in this order. For example, H0-1MD corresponds to homopolymer (H0) specimens of 1 mm thick and tested in orientation MD.

4.1. Fracture behaviour

During testing of the DDENT specimens, it has been observed that depending on the material, thickness and orientation, the fracture behaviour was different. As can be seen in Fig. 3, five different types of fracture were identified as given below.

(a) *Brittle*. There is a small plastic deformation by crazing and unstable crack propagation. This is reflected in the load–displacement curve (Fig. 4(a)) with a maximum and sudden load drop. This type of rupture was observed in H0-1TD. In this case, the EWF method is not applicable since there is no full ligament yielding before crack propagation [8].

(b) *Ductile instability*. This case is characterised by a small plastic deformation with little stress whitening near the notches. However, instead of yielding at the process zone there is an unstable propagation of the crack, producing brittle behaviour. As can be seen in Fig. 4(b), the load–displacement curve is similar to that of case (a). Crazes were not observed in this case. Our group has already reported that copolymerisation with small amounts of ethylene [15] avoids this typical phenomenon of the PP homopolymer. Actually, only the homopolymer showed this type of fracture (H0-2TD, H0-3MD and H0-3TD). As in case (a), the EWF method is not applicable.

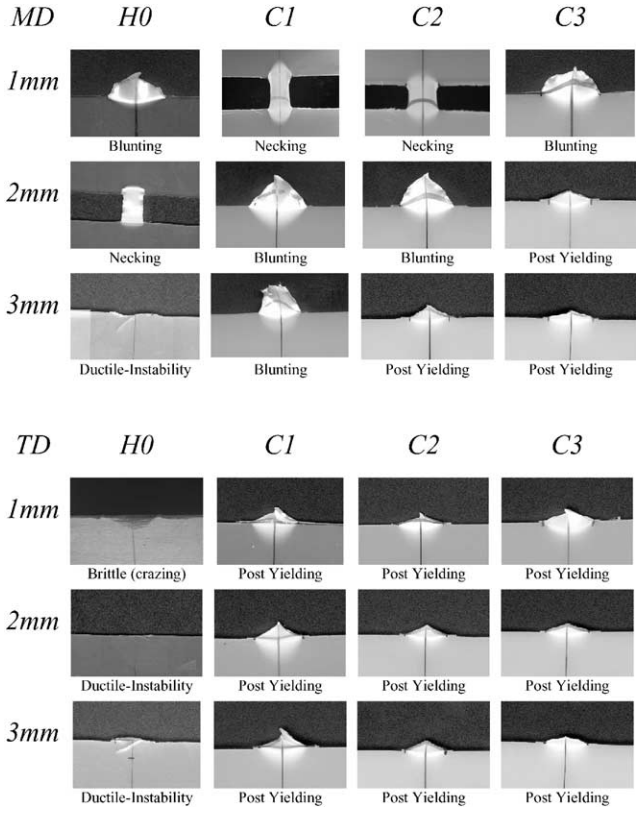

Fig. 3. Photomicrographs of the ligament of the fractured specimens as a function of test direction, thickness and material ($l \approx 14$ mm).

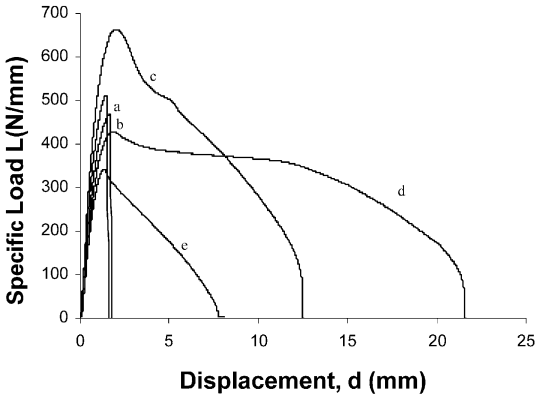

Fig. 4. Specific load (load/thickness) vs. displacement curves representatives of the different fracture behaviours: (a) Brittle (H0-1TD); (b) Ductile instability (H0-3MD); (c) Blunting (H0-1MD); (d) Necking (C2-1MD) and (e) Post-yielding (C2-1TD).

(c) *Blunting*. In this case, the process zone is fully yielded before crack growth. After yielding, the crack tip blunts strongly and it does not follow steady crack propagation. In Fig. 4(c) it can be observed that the load drop after yielding is not constant and how blunting causes a higher energy absorption in the fracture process. This behaviour was observed in H0-1MD, C1-2MD, C1-3MD, C2-2MD, and C3-1MD. The EWF method is not applicable.

(d) *Necking*. In spite of a crack propagation perpendicular to the tensile direction, the process zone yields with high plastic deformation. After this necking process, much more alike to a dumb-bell tensile test, a crack appears and propagates in one or both sides of the DDENT specimen. It can be observed that there is some tearing (indicated by arrows in Fig. 5) above the process zone, suggesting that the fracture process penetrates into the plastic zone. In Fig. 4(d), it can

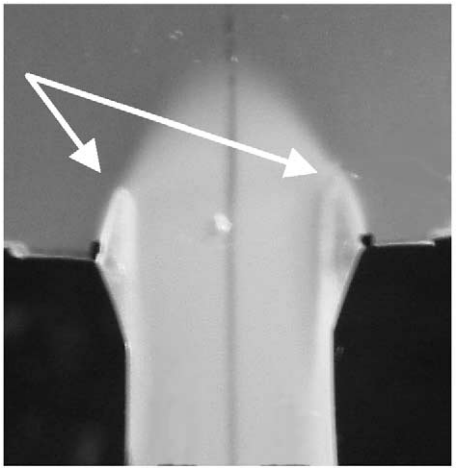

Fig. 5. Detail of a necked region of C1-1MD.

be seen that the corresponding load–displacement curve is characterised by a very smooth load drop after yielding and very high values of deformation at fracture. This type of fracture, observed in H0-2MD, C1-1MD and C2-1MD, invalidates the use of the EWF as it has been showed by several authors [13,16].

(e) *Post-yielding*. All the statements postulated to apply the EWF are observed. The crack starts at the sharpened notches after complete yielding of the process zone and propagates in a stable manner, as can be seen in the curve showed in Fig. 4(e). In these cases, the EWF method is fully applicable.

Cases (c) and (d) (blunting and necking) could be considered as two different degrees of the same phenomenon but in this work it has been preferred to treat them separately considering blunting as an intermediate case between post-yielding and necking. Although the EWF method can only be applied in the case of post-yielding, the fracture parameters obtained with other type of fracture behaviour were used in some cases for qualitative approaches.

4.2. Determination of EWF parameters

The fracture parameters were determined following the ESIS protocol for EWF. The diagrams in Fig. 6 (corresponding to material C2) are shown, as an example of all the steps needed to determine the EWF values. Similar plots were obtained for C1 and C3. Firstly, the self-similarity of the L–d curves was checked in every set of experiments, as shown in Fig. 6(a) for C2-2TD. In all cases studied, it was found that the L–d curves were alike. Afterwards, the stress levels were examined, plotting σ_{max} of the L–d curves vs. l (Fig. 6(b)). The ESIS protocol for EWF [11] suggests the application of the Hill criterion [10] as a check for the essential work data. A straight line indicates the value of $1.15\sigma_y$ obtained in tensile tests, indicating the theoretical upper value of σ_{max} under pure plane stress conditions. It is remarkable that in almost all cases, data fell below this value. This criterion was used to verify the lower limit for ligament lengths, set at first as Max($3t$, 5 mm).

Finally, the w_f vs. l (Fig. 6(c)) were plotted. It is worthwhile noting that the w_f–l diagrams gave very good linear regression coefficients in most of the cases. When blunting or necking phenomena was present, there was an increase in the scatter of the w_f–l diagrams and its subsequent increase in the standard error in the fracture values calculated.

Table 1 shows all the results obtained for EPBC. Note that the values in shadow background correspond to the cases in which not all the assumptions needed to apply the EWF were observed. The calculation of the shape factor β has not been considered because of the inaccuracy and complexity in its determination. As in other works in literature [17,18], we considered that the plastic item, βw_p, describes well enough the plastic work evolution for our purposes.

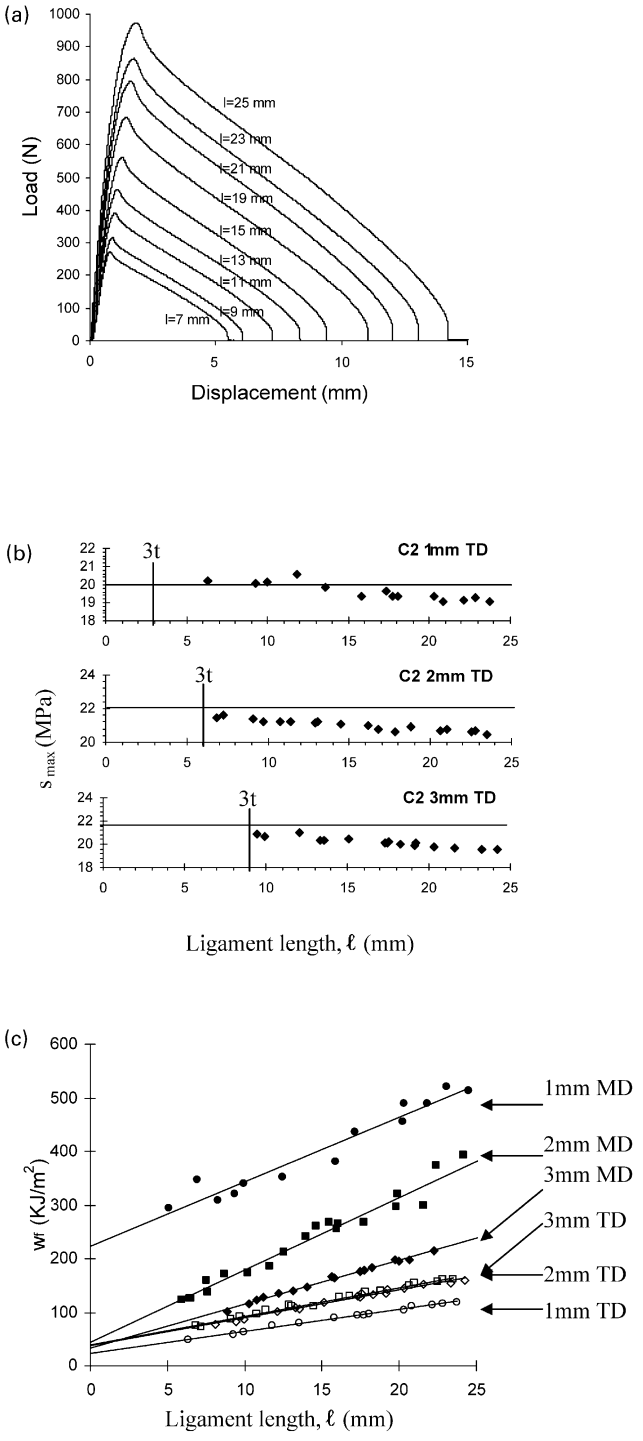

Fig. 6. Determination of EWF parameters for C2: (a) Verification of self-similarity in L–d curves. In this case, C2-2TD; (b) Application of the Hill criterion to verify the state of tensions (horizontal line represents the value $1.15\sigma_y$); (c) Diagrams w_f vs. l to determine fracture parameters by least square regression.

4.3. Effect of orientation

When tension was applied to DDENT samples in the MD direction, the fracture behaviour showed a trend to cause strong blunting, avoiding steady crack propagation. In the

Table 1
EWF parameters calculated for C1, C2 and C3. The values in shadow background must be considered as non-representative of the toughness of the material because of their fracture behaviour. The confidences have been determined as the standard deviations in the least square regression

		C1		C2		C3	
Thickness	Orientation	w_e (kJ/m^2)	βw_p (MJ/m^3)	w_e (kJ/m^2)	βw_p (MJ/m^3)	w_e (kJ/m^2)	βw_p (MJ/m^3)
1 mm	MD	380 ±60	36.9 ±4	214 ±18	13 ±1.2	32 ±5	12.1 ±0.3
2 mm	MD	103 ±14	26.0 ±0.9	44 ±9	13.5 ±0.6	25.1 ±1.3	6.34 ±0.08
3 mm	MD	77 ±14	14.4 ±0.8	33.9 ±2.6	8.14 ±0.16	32.4 ±1.9	3.47 ±0.11
1 mm	TD	16.6 ±2.4	6.45 ±0.15	25.5 ±1.9	4.49 ±0.11	21.2 ±1	2.03 ±0.05
2 mm	TD	22.0 ±4.1	7.30 ±0.25	38.7 ±2.1	5.37 ±0.13	22.2 ±2.1	3.66 ±0.13
3 mm	TD	21.6 ±3.3	7.84 ±0.2	36.3 ±2.7	5.26 ±0.16	28.2 ±2.4	3.39 ±0.13

case of the specimens tested in TD, the fracture process involved less deformation than in their homologues in MD and the fracture energies represented by the area under the L–d curves were in all cases higher in MD than in TD. Thus, the fracture behaviour in MD is more ductile than in TD.

In order to estimate qualitatively the effect of the orientation as a function of thickness and EC, all of the calculated EWF parameters (including those with shadow background in Table 1) were used. If we consider that the differences in the w_e and βw_p values between the samples tested in MD and TD are attributed only to the effect of the orientation, the trends observed indicate that:

(a) Increase of thickness reduces the effect of orientation. In Table 1 it can be observed that the differences between the w_e values in MD and TD decrease from 1 to 3 mm. The plastic term (βw_p) gives the same trend and seems to be more sensitive than w_e in thick specimens.
(b) Increase of EC decreases also the effect of orientation. Again, in Table 1 it can be noticed that fracture parameters obtained for C1 differ among them more than the ones obtained for C3.

These tendencies can be explained considering the processing induced morphology of the plaques. During the injection-moulding process, the material enters inside the cooled mould at high pressure through a small gate. This causes the polymer to crystallise under a high shear stress, especially near the surface, as described by the Tadmor model [19]. This process generates a skin/core structure, which leads to oriented higher order structures near the surface, and less oriented ones in the core. As the crystalline structures of the skin and core are different, they show different birefringence. This makes it fairly easy to visualise the skin/core structure looking through a thin section of a plaques using polarised light microscopy (PLM) [20]. Complementing this technique with Wide-angle X-ray diffraction, Fujiyama [21] revealed that in the case of PP this skin is very anisotropic due to its highly oriented structure. While the skin can be described on the basis of a shish–kebab model in which fibrous crystals oriented in MD (shishes) penetrate oriented lamellae (kebab), the core corresponds to a spherulitic structure. The skin would then act like a fibre reinforced structure, as schematically shown in Fig. 7, influencing greatly the fracture properties of the plaques.

Using PLM, it was observed that the oriented skin evolved with the increase of thickness and EC, as can be seen in Fig. 8. As thickness increases, it can be seen that either the skin to core ratio decreases because of the enlargement of the core (as in H0-1mm and H0-2mm) or the skin thickness decreases (C2-1mm and C2-2mm). This reduction of the skin is due to the differences of shear stress produced during the process of filling the mould cavity. In thicker moulds it takes place with less shear stress (in the gate and inside the mould) causing less orientation. Furthermore,

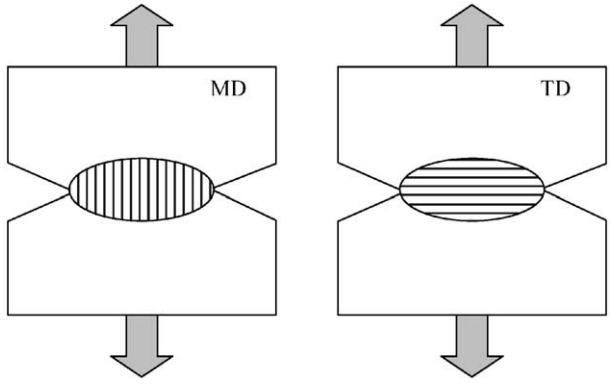

Fig. 7. Schematic representation of oriented higher order structures in DDENT samples obtained from injected plaques. The lines denote oriented fibrous crystals acting as if they were long oriented fibres.

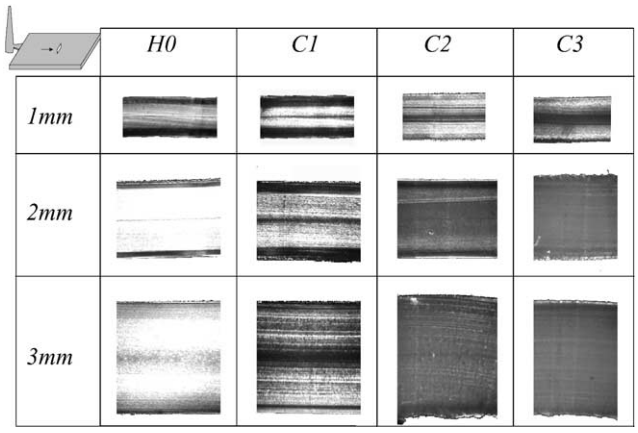

Fig. 8. PLM microphotographs taken from micro-slices of the plaque sections revealing the skin/core structure.

during cooling of the plaques the heat transfer of the core of the thicker plaques is more difficult, so it takes more time to cool down. This allows the inner chains of the skin to relax and thus lower the skin/core effect.

The EC acts in the same direction as the thickness of the plaque, lowering the skin thickness (C1-2mm and C2-2mm). The EC contributes to a higher mobility of the polymer chains lowering relaxation times and melt orientation. It results in lower orientation of the chains during cooling, reducing the skin/core effect.

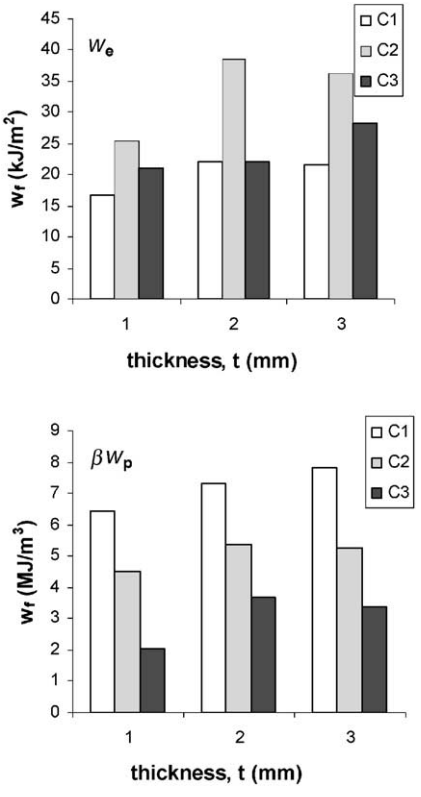

Fig. 9. EWF values as a function of thickness and EC in TD.

4.4. Effect of ethylene content

The presence of the ethylene phase in EPBC allowed the suppression of the ductile–brittle transition as it has been shown previously. These observations are in accordance with the work done by our group [14], in which we also found this phenomenon at low temperatures in thin films.

In order to discuss in detail the influence of the EC, only the EWF parameters obtained in TD will be referred. In all this values, represented in Fig. 9, the assumptions needed to apply the EWF method are achieved.

We saw that the plastic term, βw_p, decreased with higher EC. As shown in Ref. [14] at $T > T_g$ PP (which is our case), the PP blocks have no movement restrictions and they govern the plastic behaviour of the material. Therefore, as the deformation of the ethylene blocks involves less energy dissipation, the global plastic energy decreases with EC.

Unlike the plastic item, the EWF presented a maximum value for C2. Hints for an explanation may be found on the influence of crystallinity on w_e, following the Karger-Kocsis idea [7] of relating w_e to the energy needed to initiate a crack and w_p to the energy necessary to propagate it. As higher crystallinity corresponds to higher energy absorption, increase of crystallinity should be accompanied by an increase of w_e. However, high crystallinity would also reduce the number of tie molecules acting as stress-transfer units at the crack tip, causing a decrease in w_e. As both contributions act in opposite directions, the balance between them seems to be responsible for a maximum value of w_e in the case of C2 (at the present strain rate, temperature and within this range of thickness).

We suggest that a detailed study on crystalline morphology could set the basis for a reasonable interpretation of these results, and our efforts are heading to this direction.

4.5. Effect of thickness

The influence of the thickness can hardly be separated from the processing induced morphology of the plaques. Only the series tested in TD will be considered, since there are not enough valid EWF values in MD to propose a valid trend with thickness.

In TD, we observe that toughness is slightly increased with thickness since both w_e and βw_p increase from 1 to 3 mm (Fig. 9). To provide a reasonable explanation to this unusual tendency with respect to some other published works [15,22] the different fracture behaviour of the skin and core has been observed in detail. The fracture behaviour of the oriented skin of the plaques in TD cases was more brittle than the non-oriented core and, consequently, less energy-absorbent. As we have discussed previously, increase of thickness brings a reduction of the skin morphology. This results in higher energy absorption of specimens with less skin. Therefore, as the reduction of the skin morphology with thickness seems to be responsible for this tendency, it is concluded that the EWF method shows

that the thickness in this range has little influence on toughness.

5. Conclusions

Using the EWF method, it has been observed that strong interrelationships among thickness, EC and orientation greatly influence the fracture properties of EPBC plaques.

The injection-moulding process has induced diverse crystal morphologies inside the plaques causing different behaviour upon the direction of tension loading. Using PLM we have been able to attribute these differences to the presence of a skin/core structure in the plaques. The increase of both thickness and EC reduces the extent of the skin/core structure. The EWF values obtained are in agreement with the information provided by PLM.

Because of the interrelated effects of thickness and EC with the skin/core structure, it has not been possible to study independently their influence on fracture parameters. However, an effort has been made looking especially the plaques tested in TD.

In general, the presence of the EC prevented brittle behaviour of PP. The fracture parameters, w_e and βw_p, behave differently. While the plastic item decreases with increase of EC, the essential work presents a maximum value for C2. This maximum has been attributed to the effect of EC on crystallinity.

The increase of thickness in samples tested in TD resulted in small increase of toughness, attributed to the reduction of the skin structure.

Acknowledgements

The authors are grateful to the MCYT and their financial support to the project MAT2000-1112-P3 in which this work is involved. Special acknowledgement is also given to BASELL for supplying the raw materials. J. Gámez-Pérez is grateful for a doctoral grant from the MCED.

References

[1] Mai YW, Cotterell B. Int J Fract 1984;24:229.
[2] Seth RS. Tappi J 1995;78(10):177.
[3] Maspoch MLl, Santana OO, Grando J, Ferrer-Balas D, Martinez AB. Polym Bull 1997;39:249.
[4] Mai Y-W, Cotterell B, Horlyck R, Vigna G. Polym Engng Sci 1987;27:804.
[5] Wu J, Mai Y-W. Polym Engng Sci 1996;36(18):2275.
[6] Hashemi S. J Mater Sci 1997;32:1563.
[7] Karger-Kocsis J. Microstructural and molecular dependence of the work of fracture parameters in semicrystalline and amorphous polymer systems. Fracture of polymers, composites and adhesives. Oxford: Elsevier Science Ltd, 2000.
[8] Cotterell B, Reddel JK. Int J Fract 1977;13:267.
[9] Broberg KB. J Mech Phys Solids 1975;23:215.
[10] Hill R. J Mech Phys Solids 1952;1:19.
[11] Clutton E. Essential work of fracture. Fracture mechanics testing methods for polymers, adhesives and composites. Oxford: Elsevier Science Ltd, 2001.
[12] Ferrer-Balas D, Maspoch MLl, Martínez AB, Santana OO. Polymer 2001;42(4):1697.
[13] Ferrer-Balas D, Maspoch MLl, Martínez AB, Ching E, et al. Polymer 2001;42(6):2665.
[14] Ferrer-Balas D, Maspoch MLl, Mai Y-W. Polymer 2002;43:3083.
[15] Maspoch MLl, Ferrer D, Gordillo A, Santana OO. J Appl Polym Sci 1999;73:177.
[16] Karger-Kocsis J, Mouzakis DE. Polym Engng Sci 1999;39(8):1365.
[17] Ferrer-Balas D, Maspoch MLl, Martínez AB, Santana OO. Polym Bull 1999;42:101.
[18] Karger-Kocsis J, Czigány T. Polym Engng Sci 2000;40(8):1809.
[19] Tadmor Z. J Appl Polym Sci 1974;18:1753.
[20] Varga J. J Mater Sci 1992;27:2557.
[21] Fujiyama M. Higher order structure of injection-molded polypropylene. Polypropylene, structure and morphology. London: Chapman & Hall, 1995.
[22] Saleemi AS, Nairn JA. J Appl Polym Engng Sci 1990;30:211.